ARTICLE

ACS chemical biology

Identification of a Small Molecule Inhibitor of Importin β Mediated Nuclear Import by Confocal On-Bead Screening of Tagged One-Bead One-Compound Libraries

Martin Hintersteiner[†,§,∥], Géza Ambrus[‡,∥], Janna Bednenko[‡], Mario Schmied[§], Andrew J. S. Knox[†], Nicole-Claudia Meisner[§], Hubert Gstach[§], Jan-Marcus Seifert[§], Eric L. Singer[‡], Larry Gerace[‡,*], and Manfred Auer[†,§,*]

[†]The University of Edinburgh, School of Biological Sciences (CSE) and School of Biomedical Sciences (CMVM), CH Waddington Building, 3.07, The King's Buildings, Mayfield Road, Edinburgh EH9 3JD, U.K. and [‡]Department of Cell Biology, The Scripps Research Institute, 10550 N. Torrey Pines Road, La Jolla, California 92037, [§]Affiliation when work was performed: Innovative Screening Technologies unit, Novartis Institutes for BioMedical Research (NIBR), Brunnerstrasse 59, A-1235 Vienna, Austria. [∥]These authors contributed equally to this work.

ABSTRACT In eukaryotic cells, proteins and RNAs are transported between the nucleus and the cytoplasm by nuclear import and export receptors. Over the past decade, small molecules that inhibit the nuclear export receptor CRM1 have been identified, most notably leptomycin B. However, up to now no small molecule inhibitors of nuclear import have been described. Here we have used our automated confocal nanoscanning and bead picking method (CONA) for on-bead screening of a one-bead one-compound library to identify the first such import inhibitor, karyostatin 1A. Karyostatin 1A binds importin β with high nanomolar affinity and specifically inhibits importin α/β mediated nuclear import at low micromolar concentrations *in vitro* and in living cells, without perturbing transportin mediated nuclear import or CRM1 mediated nuclear export. Surface plasmon resonance binding experiments suggest that karyostatin 1A acts by disrupting the interaction between importin β and the GTPase Ran. As a selective inhibitor of the importin α/β import pathway, karyostatin 1A will provide a valuable tool for future studies of nucleocytoplasmic trafficking.

The nuclear envelope (NE) of eukaryotic cells is the membrane barrier that separates the nuclear events of DNA replication and mRNA biogenesis from cytoplasmic processes such as protein production and metabolism (*1, 2*). Nucleocytoplasmic communication involves bidirectional, signal-dependent transport of RNAs and proteins across the NE through the nuclear pore complexes (NPCs), which are ~100 MDa protein assemblies comprising multiple copies of ~30 nucleoporins (Nups). Macromolecular trafficking across the NPC is mediated by transport receptors called karyopherins, or importins and exportins (*3, 4*), which typically recognize linear stretches of amino acids called nuclear localization sequences (NLSs) and nuclear export sequences (NESs) on their protein cargoes. The β karyopherin protein family has >20 members in vertebrates, including the exportin CRM1 and the importins importin β and transportin (*5*).

Importin α/β mediated nuclear import first involves recognition of NLSs by the adaptor importin α and binding of the latter to importin β through its N-terminal IBB domain (*6*). Subsequently the ternary cargo/receptor complex moves through the NPC *via* repeated transient interactions of importin β with phenylalanine-glycine (FG) repeat motifs present on certain Nups, culminating with its binding to Nup153 on the nucleoplasmic side of the NPC. Here, complex dissociation is thought to occur by the binding of RanGTP to importin β, which

*Corresponding authors, manfred.auer@ed.ac.uk, lgerace@scripps.edu.

Received for review April 10, 2010 and accepted July 30, 2010.

Published online August 2, 2010

10.1021/cb100094k

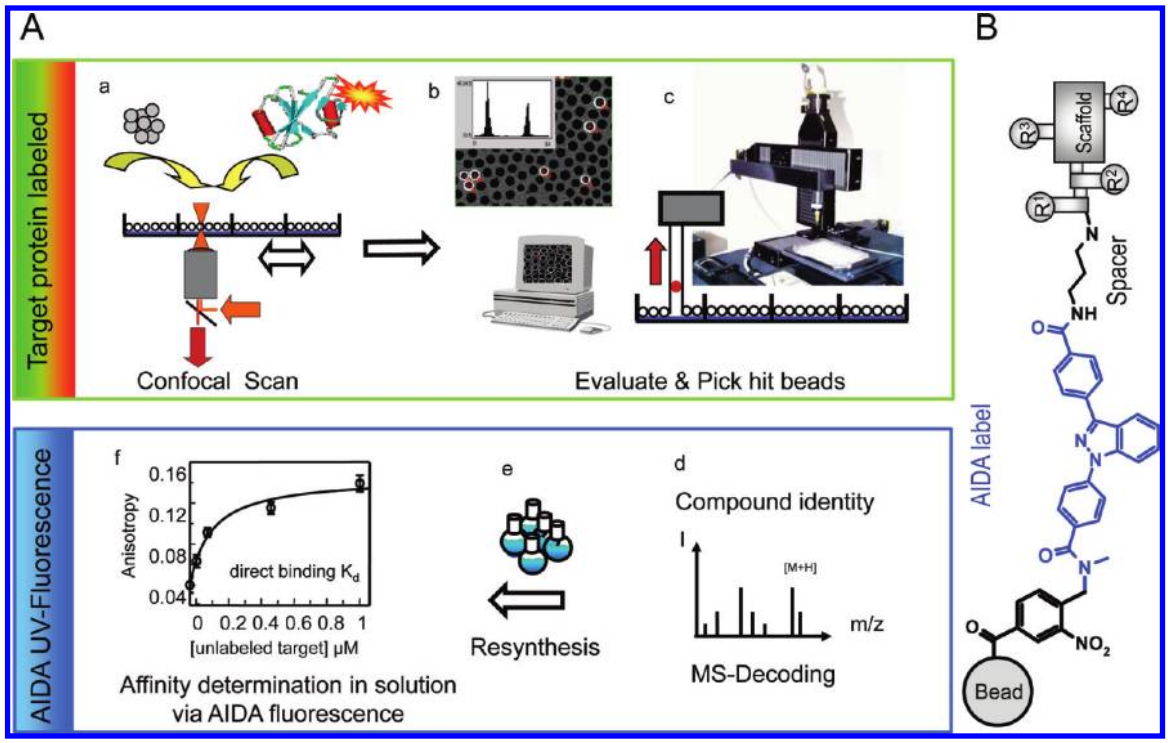

Figure 1. Affinity-based screening of AIDA-tagged one-bead one-compound libraries by confocal nanoscanning (CONA) and fluorescence based secondary assays. A) The screening process is performed in six steps (a—f): (a) Starting with distribution of 1 mg of resin from each AIDA-tagged sublibrary into the wells of a 96-well microtiter plate, followed by incubation with fluorescently tagged target protein. (b) Automated confocal nanoscanning (CONA) identifies relevant hit beads where the target protein has bound to compounds on the bead surface. (c) Hit beads are isolated by the bead-picking device of the CONA screening instruments and the compounds are cleaved from the resin. (d) MS analysis of the hit compounds allows structure assignment for each hit bead. (e) The identified hits are resynthesized in milligram quantities with and without the AIDA tracer. f) The fluorescence from the UV dye AIDA is used in a generic secondary assay to quantify the affinity of the hit compounds for the target protein and for compound ranking. Note: This process falls into two phases, a phase where the green-red fluorescence on the target protein is first used to identify hits by on-bead screening (green box) and a second phase where the UV signal from the tracer molecule is used quantify the obtained primary hits in a generic secondary assay (blue box). B) Library setup: one-bead one-compound libraries were synthesized on 90 µm TentaGel beads, using a photocleavable linker as attachment site (black), followed by a chemically robust UV tracer "AIDA" (blue), a 3-carbon atom spacer (black), and the actual screening compound. The screening compounds are built around a central scaffold, decorated with four combinatorial sites. According to the split-mix-and-divide synthesis protocol used, the last two combinatorial sites are identical for each compound in any one sublibrary.

causes release of the IBB domain by an allosteric mechanism (*7*). The RanGTP—importin β complex then translocates into the cytoplasm, and upon GTP hydrolysis, importin β is released for another round of nuclear import. The directionality of nuclear import is defined by nucleocytoplasmic compartmentalizion of the GEF (guanine exchange factor) and GAP (GTPase activating protein) that regulate the nucleotide state of Ran, with GTP hydrolysis providing the underlying energy that drives cargo concentration (*2, 8*).

Confocal nanoscanning (CONA) is an automated screening method developed for large one-bead one-compound libraries (Figure 1) (*9*). In this method, the binding of a fluorescently labeled protein to bead-immobilized compounds is quantitatively detected with high optical resolution by large area confocal scanning of a bead monolayer in the wells of a microtiter plate. Beads that are positive for binding are retrieved from the plate by bead-picking with a robotic driven capillary. The compounds containing the UV dye 4-{3-{4-[(3-aminopropyl)-aminocarbonyl]-phenyl}-1*H*-indazol-1yl}-benzoic acid (AIDA) as a tag are then cleaved from the beads, their identity is confirmed by mass spectrometry, the compounds are resynthesized, and used for bind-

ing studies utilizing the AIDA fluorescence. Fluorescence intensity profile analysis of beads offers high sensitivity detection of target protein-compound interactions on the bead surface and allows the exclusion of beads with strong autofluorescence. AIDA does not interfere with visible range fluorescent dyes and has a distinctive fragmentation pattern in MS that facilitates decoding of hit compounds.

The identification of CRM1 (exportin 1) as the protein target for the potent antitumor natural product leptomycin B (LMB) has spurred substantial interest in targeting the nuclear export and import machinery for drug discovery (*10–15*). LMB also has proved to be extremely useful for the analysis of nucleocytoplasmic transport of hundreds of endogenous, as well as viral proteins (*16, 17*). Recent work describes additional small molecules that target CRM1 and inhibit nuclear export, specifically *N*-acetylacrylates (*18*). Also, a high affinity substrate-like peptide of 26 amino acids has been developed recently that binds to importin α and inhibits importin α/β mediated nuclear import and cell growth (*19*). However, to date no small molecule inhibitors of nuclear import have been described.

Here, we have identified a cohort of importin β-binding small molecules with a CONA screen. From this group, we have characterized one compound that selectively inhibits the importin α/β pathway in permeabilized and live cell nuclear import assays. We provide evidence that this compound, which we term karyostatin 1A, may function by inhibiting the binding of RanGTP to importin β. This compound should be useful for future structural and functional studies of nuclear import.

RESULTS AND DISCUSSION

On-Bead Screening by Confocal Nanoscanning (CONA). Importin β is a major β-karyopherin whose interactions with several components of the nuclear import machinery have been biochemically and structurally characterized. To explore the potential of inhibiting importin β function with small molecule high affinity binders, we performed a CONA on-bead screen (Figure 1) with Alexa-488 labeled importin β (*9, 20–23*). (Protein labeling and characterization are described in the Supporting Information text and in Supplementary Figures S1−S4). We screened a 45,600 compound containing diversity-optimized subset from our much larger stock of one bead, one compound libraries (2.2 million compounds). The screened compound collection consisted of 96 sublibraries, each containing approximately 500 members, and each of which was based on heterocyclic scaffolds such as pyrroles, thiazoles, indoles, amino-prolines, *etc.* All compounds from one individual sublibrary contain the same building block in the last two combinatorial positions (R3 and R4; Figure 1, panel B; Supplementary Figure S5).

Using 60 nM Alexa-488 labeled importin β for the bead incubation, on-bead screening by CONA detected 928 hit beads, corresponding to a rather high hit rate of 2% (Figure 2, panel A). The hits were clustered in sublibraries containing two scaffolds: pyrroles and 4-aminoprolines. All hit beads were ranked according to the intensity of fluorescently labeled target protein bound to the compounds on the bead surface (Figure 2, panels B and C). The 235 top ranked beads were then isolated using the bead picking feature of the PickoScreen instrument (Supplementary Table S1 and Figure S6); 153 of these contained pyrrole compounds and the remaining 82 hit beads came from 4-aminoproline sublibraries. Using HPLC-MS^2 based structure elucidation, compound structures were successfully assigned to all isolated hit beads (Supplementary Figures S7 and S8). Moreover, in the pyrrole subset, 17 compounds were identified twice (doublet), 7 compounds three times (triplet), and 1 compound four times (quadruplet), leaving 96 unique structures. The aminoproline subset of beads contained only 5 duplicates and 72 unique structures. Building block frequency analysis revealed a strong preference for either arginine or 4-aminoproline in the second combinatorial position (R2; Figure 1, panel B) of the pyrrole hits and no clear preference in the first combinatorial position (R1; Figure 1, panel B) (Supplementary Figure S9). The same building block frequency analysis for aminoprolines showed a preference for benzylamine in the first combinatorial position and a slight preference for chlorobenzylsulfonyl residues in the second combinatorial position (Supplementary Figure S9). On the basis of these decoding results, we resynthesized larger quantities of four pyrrole and three amino-proline AIDA/non-AIDA compound pairs, *i.e.*, hit compounds with AIDA (compounds **1**, **3**, **5**, **7**, **9**, **11**, **13**; designated Iβ1A to Iβ7A) and without AIDA (compounds **2**, **4**, **6**, **8**, **10**, **11**, **14**; designated Iβ1N to Iβ7N) (Figure 3; syntheses and characterization are described in the Supporting Information).

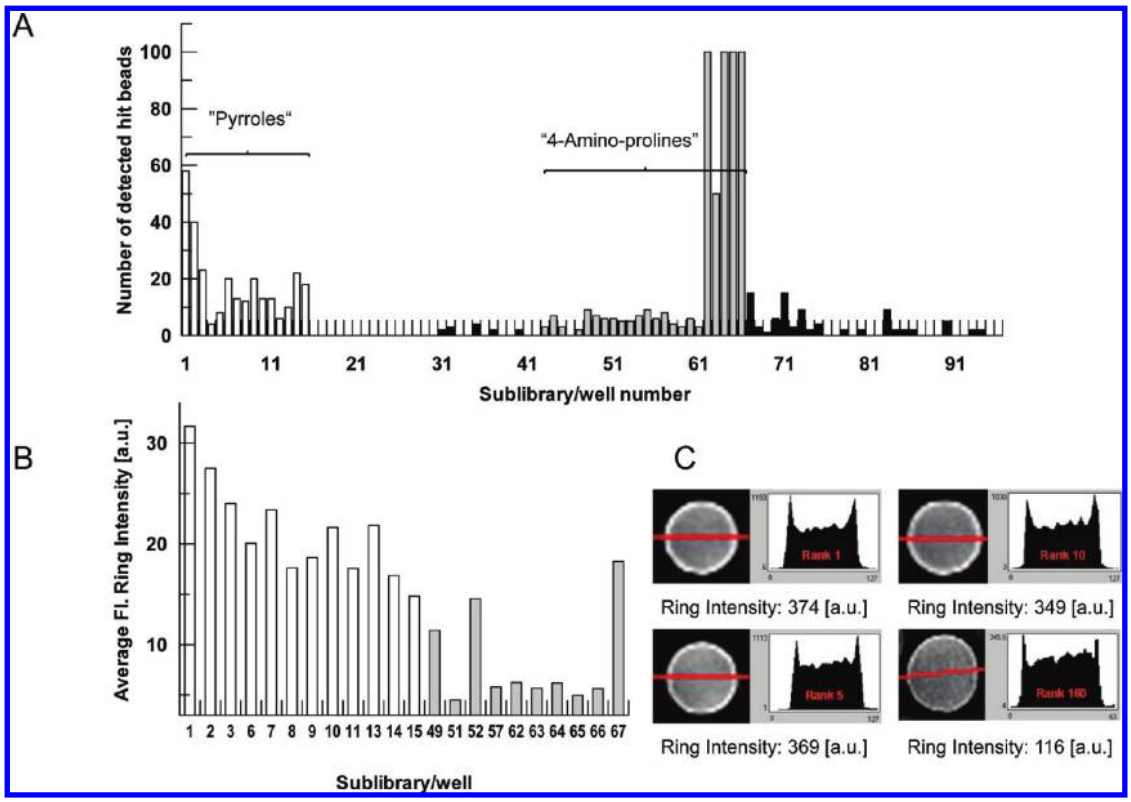

Figure 2. Primary on-bead screening analysis. A) Distribution of the number of hit beads over one 96-well screening plate containing a diversity optimized subset of AIDA-tagged one-bead one-compound libraries. Each well number represents one sublibrary. B) Quantitative analysis of relative fluorescence ring intensities of hit beads from pyrrole and amino-proline containing wells. Fluorescence ring intensity is the quantitative parameter indicating the amount of fluorescently tagged target protein that has bound to the bead-immobilized compounds. C) Four exemplary bead images with their corresponding fluorescence ring intensities and ranking.

Confirmation of Identified Hit Compounds. In a first confirmation step, we used the AIDA fluorescence of compounds Iβ1A to Iβ7A for measuring their affinities (K_d) for unlabeled importin β by fluorescence anisotropy (Figure 4). Using an average value of 0.73 mL g^{-1} for the specific protein and compound volume, the calculated start (free) and end (protein bound) anisotropy values for compounds Iβ1A to Iβ7A were 0.06 and 0.25, respectively (Figure 4, panel B; Supporting Information). The experimentally observed starting anisotropy values for compounds Iβ1A to Iβ7A were in good agreement with calculated values. Nonlinear curve fitting based on a 1:1 binding stoichiometry of the fluorescence anisotropy titration data resulted in K_d values ranging from 320 ± 80 nM to 1.3 ± 0.1 μM for the pyrrole compounds Iβ1A to Iβ4A (Figure 4, panel A). The affinities of the 4-aminoproline compounds Iβ5A to Iβ7A were generally higher and the determined K_ds ranged from 60 ± 20 nM to 140 ± 30 nM. Two unrelated control compounds, containing AIDA and the spacer unit, were also tested in the direct binding assay and did not produce any measurable affinity up to 4 μM of importin β (Supplementary Figure S11).

In an attempt to measure the binding of the non-AIDA tagged compounds to importin β, we carried out competition titrations with the non-AIDA tagged compounds Iβ1N to Iβ7N. However, technical difficulties precluded robust conclusions from this method. When the binding of importin β to the AIDA tagged compounds Iβ1A to Iβ7A was monitored in the presence of increasing amounts of the untagged compounds Iβ1N to Iβ7N, aggregation effects were observed at compound concentrations higher than 100 μM. In addition, high concentrations of non-AIDA compounds Iβ1N to Iβ7N

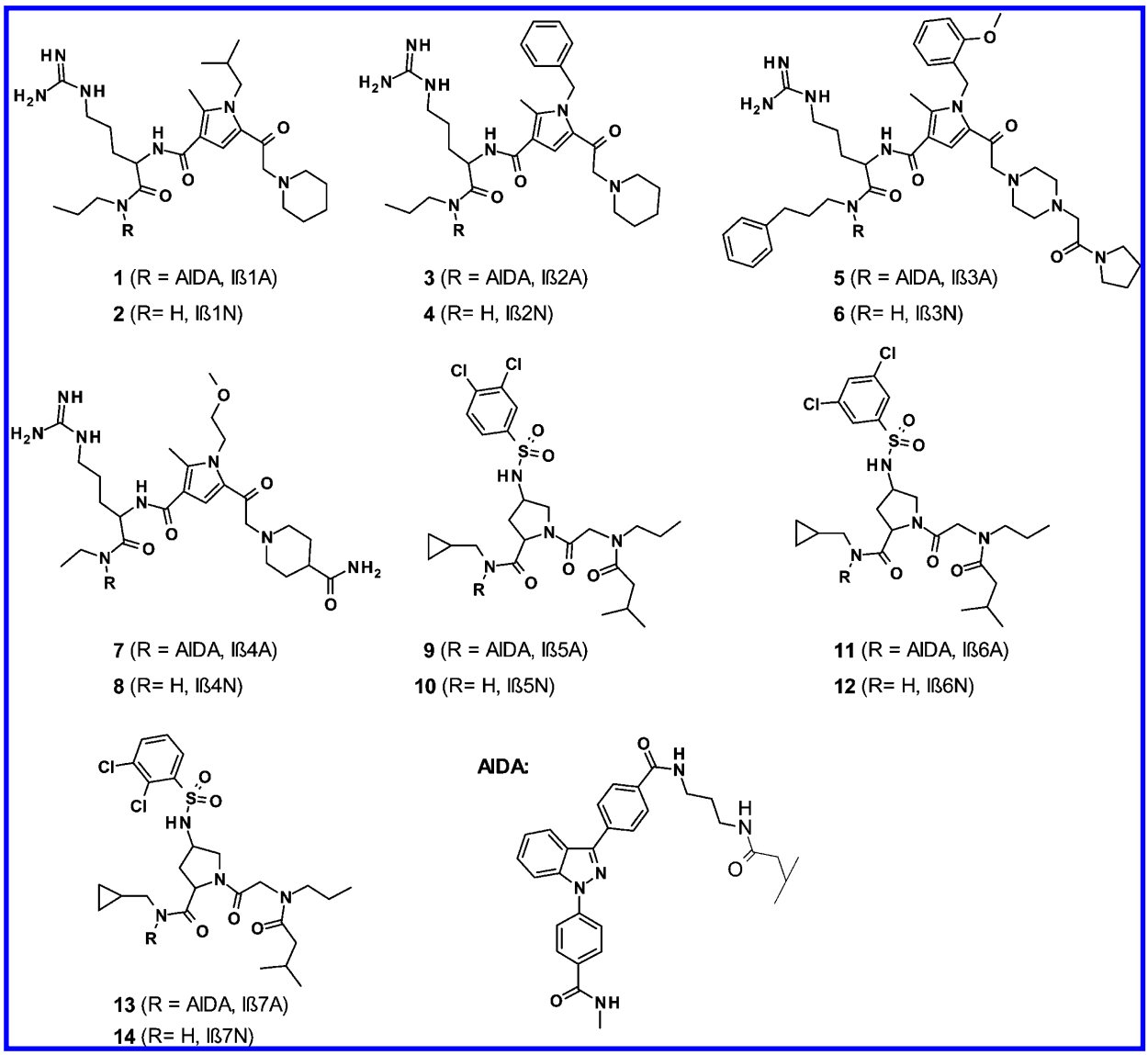

Figure 3. Resynthesized CONA derived hit compounds for importin β. On the basis of the MS analysis of the individual hit compounds and the building block frequency analysis, seven hit compounds were selected for resynthesis with (Iβ1A to Iβ7A) and without the AIDA tag (Iβ1N to Iβ7N) for further investigations in follow-up assays.

yielded autofluorescence signals, further impairing a quantitative interpretation.

However, the activities of the AIDA-tagged compounds Iβ1A to Iβ7A were further confirmed by an adaptation of a previously described size-exclusion chromatography assay (*24*), in which compounds Iβ1A to Iβ7A were centrifuged through a size-exclusion matrix in the presence or absence of importin β. The compound concentration in the filtrate after centrifugation was determined by HPLC (Figure 4, panel C). For all seven resynthesized compounds, the recovery in the presence of importin β consistently exceeded the recovery without protein. The three 4-aminoproline compounds, moreover, showed higher recoveries (more than 68%) as compared to those of the pyrrole compounds (1−5%).

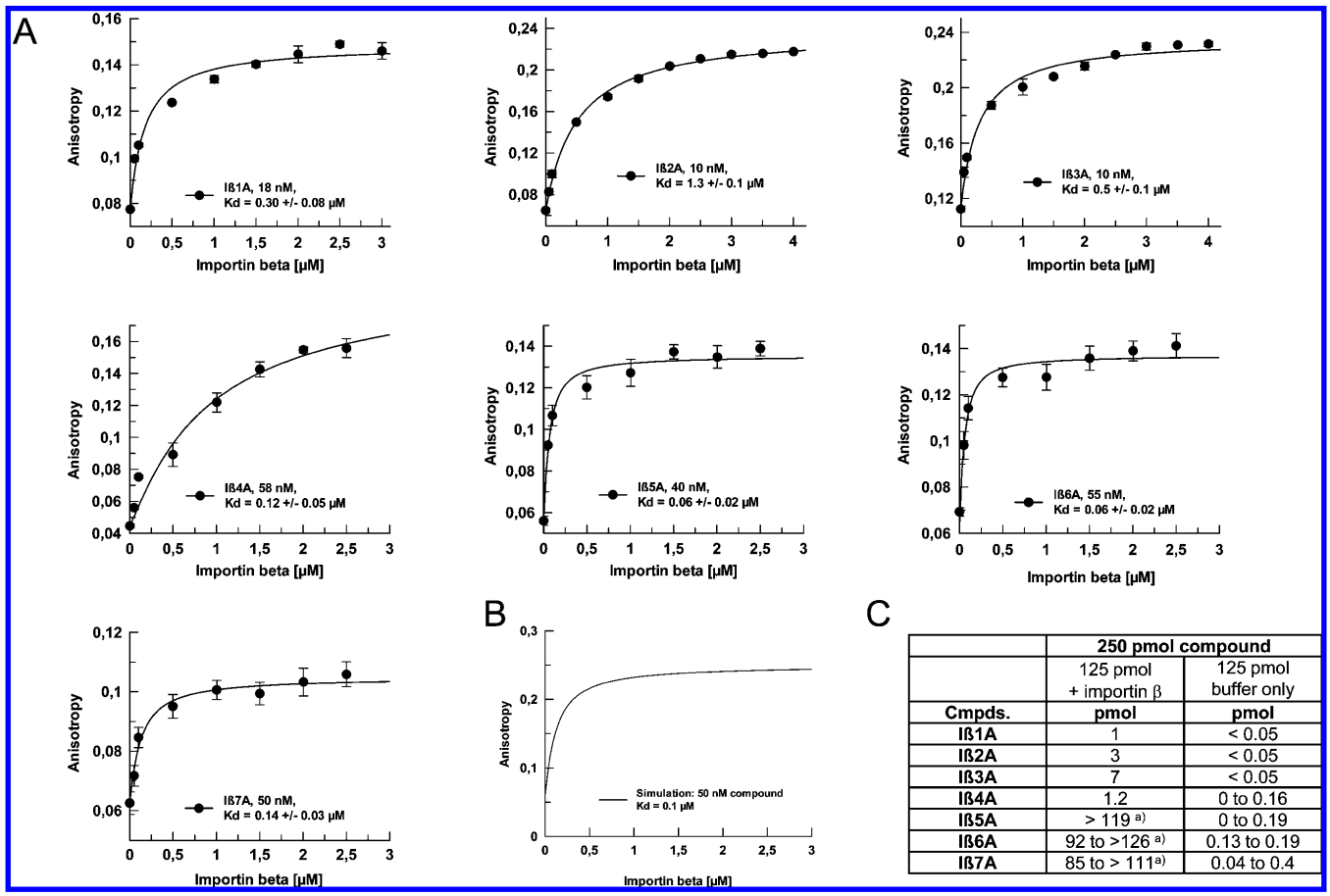

	250 pmol compound	
	125 pmol + importin β	125 pmol buffer only
Cmpds.	**pmol**	**pmol**
Iß1A	1	< 0.05
Iß2A	3	< 0.05
Iß3A	7	< 0.05
Iß4A	1.2	0 to 0.16
Iß5A	> 119 [a)]	0 to 0.19
Iß6A	92 to >126 [a)]	0.13 to 0.19
Iß7A	85 to > 111[a)]	0.04 to 0.4

Figure 4. Determination of binding affinities (K_ds) of hit compounds Iβ1A to Iβ7A for importin β. A) Anisotropy measurements using the AIDA-derived fluorescence signal were carried out with increasing concentrations of importin β. The resulting titration data was fitted to a 1:1 interaction model. B) Simulation of expected start and end anisotropy values for a ligand with a molecular weight of 1,000 Da and a globular-shaped protein of 100 kDa, using the Perrin equation. C) HPLC-quantified recoveries of AIDA-tagged hit compounds after size-exclusion chromatography experiments in the presence and absence of a saturating amount of importin β.

Iβ1A to Iβ4A Specifically Inhibit Importin α/β Mediated Nuclear Import *in Vitro*. We next examined whether the importin β binding compounds Iβ1A to Iβ7A inhibited importin β mediated nuclear import *in vitro*. These compounds, along with the non-AIDA compounds Iβ1N to Iβ7N, were tested in an assay involving permeabilized HeLa cells reconstituted with recombinant transport factors and FITC labeled NLS-conjugated BSA (FITC-BSA-NLS), an importin α/β dependent cargo (*25*). The AIDA-conjugated pyrrole compounds Iβ1A to Iβ4A, when tested at a concentration of 10 μM, inhibited importin β mediated nuclear import by 36−79% (Figure 5, panel A). However, neither the AIDA-tagged 4-aminoproline compounds Iβ5A to Iβ7A nor the non-AIDA compounds Iβ1N to Iβ7N showed significant inhibition of nuclear import (Figure 5, panel A). Thus, AIDA seems to be an integral part of the pharmacophore of the importin β inhibitors Iβ1A to Iβ4A, in contrast to similarly identified HuR binding compounds (*21*). The amino-proline compounds Iβ5A to Iβ7A, which do not inhibit import, might bind to importin β in a manner that does not perturb the transport functions measured in this assay. Alternatively, the higher hydrophobicity of the amino-proline compounds as compared to the pyrroles might cause sequestration of the former in the assay by binding to other cellular components.

We examined the concentration dependence for inhibition of importin α/β mediated nuclear import by the

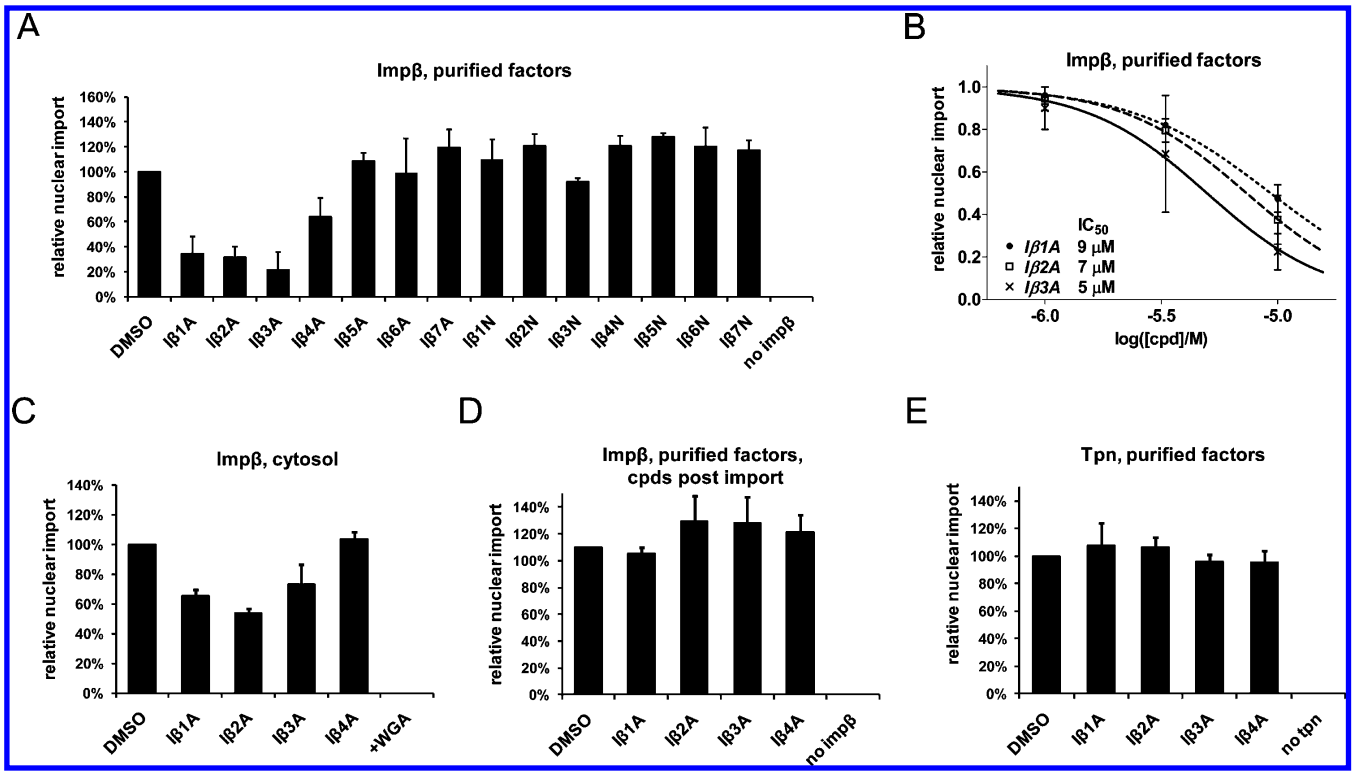

Figure 5. Effect of compounds Iβ1A to Iβ4A on *in vitro* nuclear import using permeabilized cells. Importin α/β mediated *in vitro* nuclear import using recombinant transport factors. Transport factors were added to permeabilized HeLa suspension cells together with cargo, energy, and compounds. DMSO concentration was kept at 1% across the samples. Following a 30-min reaction, nuclear fluorescence was analyzed by flow cytometry. The data points represent the average of 3−7 independent experiments. A) Compounds Iβ1A to Iβ7A and Iβ1N to Iβ7N were added at 10 μM final concentration together with FITC-BSA-NLS cargo and recombinantly expressed transport factors. B) Compounds Iβ1A to Iβ3A were added at 10, 3.3, and 1 μM concentrations with FITC-BSA-NLS cargo and recombinantly expressed transport factors. C) Compounds Iβ1A to Iβ4A were added at 10 μM final concentration together with FITC-BSA-NLS cargo and cytosol as a source of nuclear transport factors. WGA: wheat germ agglutinin. D) Nuclear import assay with FITC-BSA-NLS cargo and recombinantly expressed transport factors. Compounds Iβ1A to Iβ4A were added at 10 μM final concentration only after the nuclear import reactions were terminated by hexokinase/glucose, followed by 30 min of incubation at 30 °C to test for the loss of intranuclear FITC-BSA-NLS. E) Transportin mediated nuclear import using recombinant transport factors. Compounds Iβ1A to Iβ4A were added at 10 μM final concentration to permeabilized HeLa suspension cells together with FITC-M9-nucleoplasmin cargo.

three most active compounds Iβ1A to Iβ3A and found IC_{50} values ranging from 5 μM to 9 μM (Figure 5, panel B). We also examined transport inhibition in permeabilized cells reconstituted with cytosol instead of recombinant transport factors. In this case, significant inhibition of importin α/β mediated nuclear import by 10 μM compound was observed for Iβ1A to Iβ3A (27−46% inhibition) but was not seen for Iβ4A. The weaker inhibition in this assay might be due to additional promiscuous interactions of these compounds with other cytosolic components (Figure 5, panel C).

We also determined that inhibition of cargo accumulation with Iβ1A to Iβ4A does not result from nonspecific effects on the permeability barrier of the NE, since addition of the compounds following a nuclear import reaction did not lead to a reduction in the level of imported cargo (Figure 5, panel D). The effect of Iβ1A to Iβ4A on transportin mediated nuclear import was also examined. Transportin, although structurally similar to importin β, recognizes different cargoes, such as the M9 sequence comprising the NLS of hnRNP A1. Despite the homology of the nuclear import receptors transportin and importin β, none of the four compounds Iβ1A to Iβ4A inhibited transportin-mediated nuclear import at a compound concentration of 10 μM in the permeabilized cell nuclear import assay using recombinant transport

factors (Figure 5, panel E). This suggests that pyrrole compounds Iβ1A to Iβ4A target importin β specifically rather than the Ran system, which underlies all karyopherin-mediated nucleocytoplasmic transport.

Structure−Activity Relationships. The frequency with which a specific building block occurred in a combinatorial position within the primary hit structures gave a first indication of structure−activity relationships for the identified hit compounds. On the basis of these results, we designed and tested a set of 10 additional pyrrole compounds, Iβ8A to Iβ18A, containing a variety of residues in the four combinatorial positions (Supplementary Figure S10). Five of these were strong inhibitors (>50% inhibition) in the *in vitro* nuclear import assay and confirmed the dominant role of arginine in the second combinatorial position already seen from set of primary hits. An *N*-ethylcyclohexylamine in the fourth combinatorial position proved to be a second crucial element. (For more detailed interpretation of the SAR results, see Supporting Information.)

Iβ1A Inhibits Importin α/β Mediated Nuclear Import in Living Cells. Iβ1A, the pyrrole compound exhibiting the best combination of solubility and *in vitro* inhibitory characteristics, was further tested in living cells for its effects on the nuclear import and export of a well-characterized karyopherin cargo, green fluorescent protein fused to nuclear factor of activated T-cells (GFP-NFAT) (*26, 27*) (Figure 6, panel A). Twenty-four hours after the induction of its expression, GFP-NFAT had accumulated to substantial levels in the cytoplasm of HeLa cells (Figure 6, panel B). Nuclear import of GFP-NFAT was induced by the addition of ionomycin. After 30 min, GFP-NFAT localized to the nucleus in close to 100% of the cells (Figure 6, panel B). DMSO or 25 μM Iβ1A were then incubated with cells for 3 h, and subsequently, nuclear export was induced by incubating cells with medium lacking ionomycin but containing either 25 μM Iβ1A or DMSO for 30 min. GFP-NFAT was exported to the cytoplasm in the presence of Iβ1A as completely as with DMSO (Figure 6, panel C). Ionomycin was then readministered to the same cells. In the presence of 25 μM Iβ1A, there was inhibition of the reimport of GFP-NFAT in about 80% of the cells but not in the control (Figure 6, panel D). Together, these data show that 25 μM Iβ1A significantly inhibits importin α/β mediated nuclear import but not CRM1 mediated nuclear export of GFP-NFAT in living cells. We cannot, however, exclude the possibility that Iβ1A interferes with one or more of the other members of the β-karyopherin family *in vivo*.

Concentrations higher than 25 μM of Iβ1A (50−100 μM) triggered Iβ1A aggregation and precipitation in the cell culture medium. Lower concentrations of Iβ1A yielded weaker inhibition of nuclear import. Inhibition was seen in about 22% of the cells at 12.5 μM compound but was not seen at 6.2 μM and 3.1 μM Iβ1A (data not shown). We also analyzed compound Iβ3A in this assay but because of its lower solubility, no inhibitory effect could be detected at any tested concentration (data not shown).

Iβ1A Disrupts the Binding of Importin β to RanGTP. To rationalize the mode of action of our compounds and the observed SAR, we performed molecular modeling and docking studies with the best compound, Iβ1A. First, possible binding sites were identified using the program STP (http://opus.bch.ed.ac.uk/stp) and a computational protocol was designed to probe possible binding orientations of Iβ1A using FRED (http://www.eyesopen.com/), followed by fully flexible docking with RosettaLigand (http://www.rosettacommons.org/). The only suitable small molecule binding site, identified by STP, is located on a region of importin β where both importin α and RanGTP bind (Figure 7, panel A). According to the docking results, Iβ1A makes crucial π-stacking interactions with Trp430 as well as forming a series of hydrogen bonds; most notably, the arginine in Iβ1A interacts with Glu530 in importin β, explaining the preference observed for this specific residue in the second combinatorial position (Figure 7, panels B and C).

Inspired by the docking studies, we turned to surface plasmon resonance (SPR) for measuring the effect of Iβ1A on the interaction of importin β with three of its binding partners (GST-tagged): a Ran mutant incapable of GTP hydrolysis (RanQ69LGTP), the C-terminal region of Nup153 (amino acids 895−1475), and the IBB (Importin Beta Binding) domain of importin α (Figure 7, panels D and E and Supplementary Figures S12 and S13). GST-RanQ69LGTP, GST-Nup153, and GST-IBB were noncovalently immobilized on a Biacore sensor chip containing surface bound GST antibody. In the absence of Iβ1A, importin β bound to all three of its binding partners. The apparent K_ds measured in the SPR experiments were about 1 order of magnitude higher than previously published values (*28–30*). We attribute this to the requirement for omitting strong reducing agents from the SPR assay and the oxidation-sensitive nature

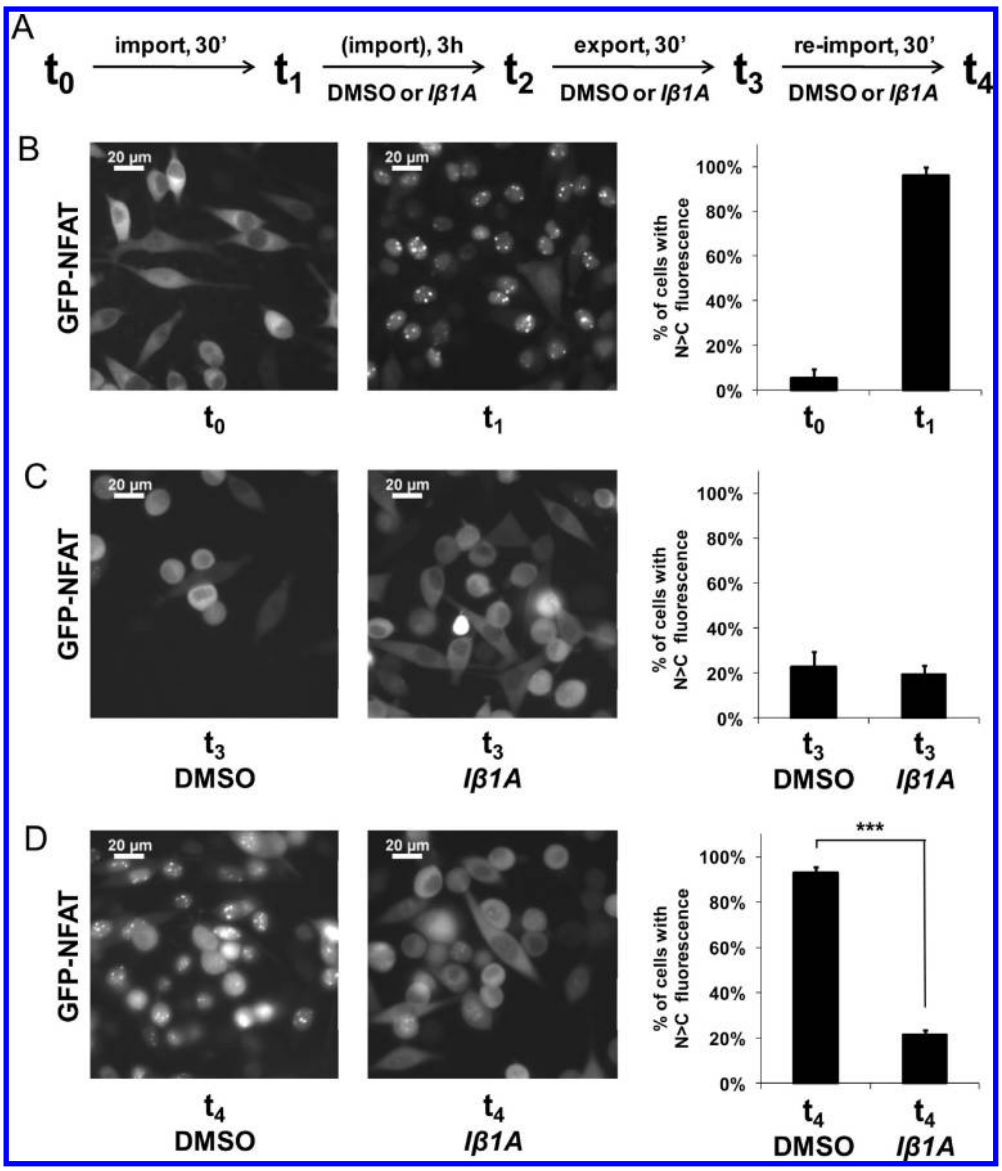

Figure 6. Effect of Iβ1A on nucleocytoplasmic export and import of GFP-NFAT in living cells. A) Schematic representation of the experimental timeline to test the *in vivo* effect of Iβ1A on nuclear export and import of GFP-NFAT in HeLa cells. "Import" or "re-import" denotes conditions where nuclear import of GFP-NFAT is triggered with the addition of 1 μM ionomycin to the cells. "Export" denotes conditions where the ionomycin is washed out with cell culture medium. B) Cytoplasmic localization of GFP-NFAT from untreated, stably transfected HeLa cells and its nuclear translocation 30 min after inducing import. C) Localization of GFP-NFAT in the presence of either 0.25% DMSO or 25 μM Iβ1A 30 min after nuclear export was induced. A 3-h incubation period with DMSO or Iβ1A in the presence of ionomycin preceded the initiation of export. D) Localization of GFP-NFAT in the presence of either 0.25% DMSO or 25 μM Iβ1A 30 min after nuclear reimport of GFP-NFAT was induced with ionomycin on the same cells that underwent export in panel C. Images in panels B–D were collected of HeLa cells expressing GFP-NFAT by fluorescence microscopy. The graphs depict the percentage of cells with predominantly nuclear GFP-NFAT, as determined by visual inspection of at least 200 cells for each condition.

of importin β (*31, 32*). The activity of importin β with our experimental conditions was nonetheless suitable for evaluating the effects of Iβ1A on binding to the various ligands. While Iβ1A at a concentration of 5 μM had

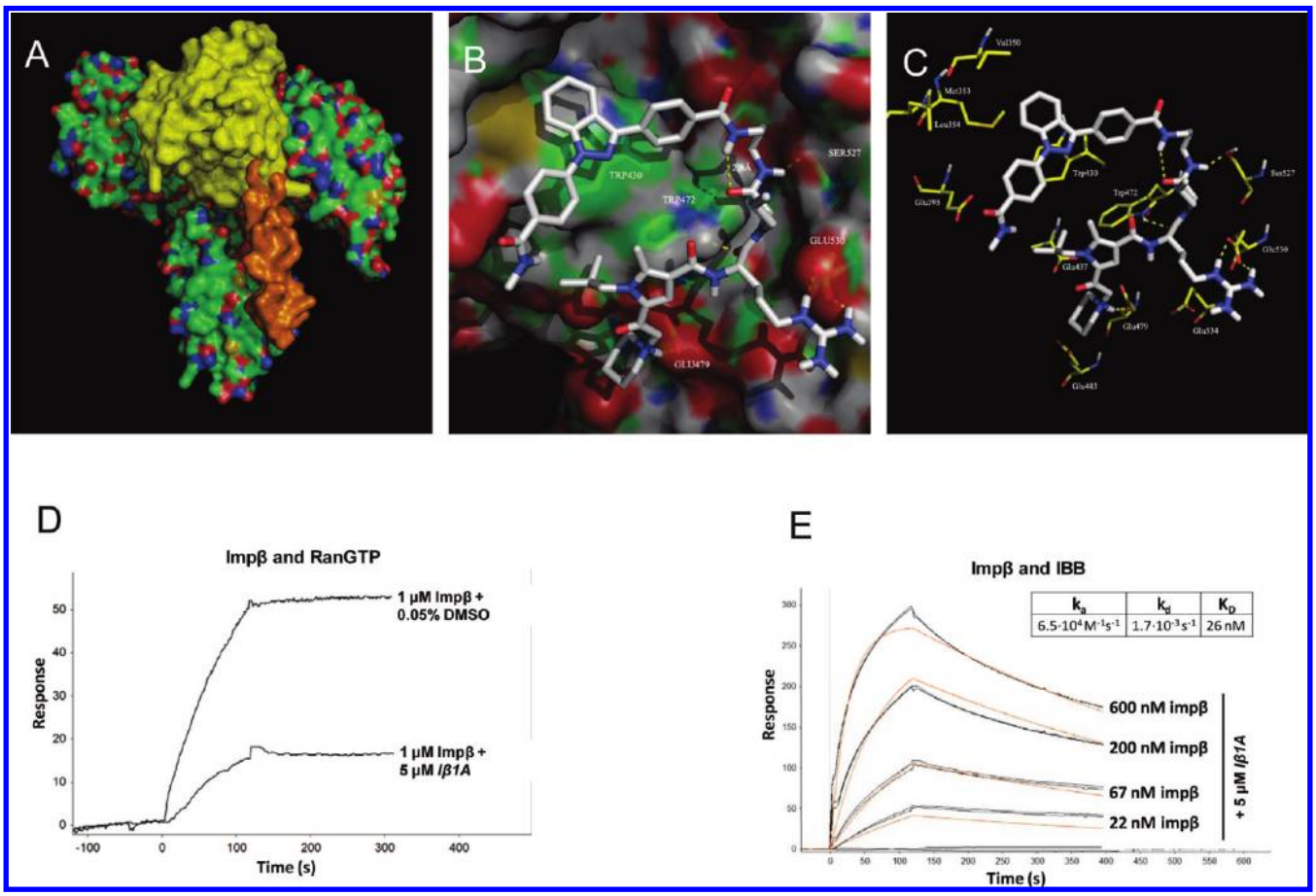

Figure 7. Molecular modeling and surface plasmon resonance measurements of the Iβ1A-importin β interaction. A) Interaction between importin β (green, colored by atom type), importin α (orange), and Ran-GTP (yellow). B) Docked structure of Iβ1A within its identified binding site. Importin β as obtained by fully flexible protein−ligand docking using the program RosettaLigand (http://www.rosettacommons.org/). C) Pharmacophore model derived from fully flexible molecular docking studies. D) Binding of importin β at 1 μM concentration to GST-RanQ69LGTP noncovalently immobilized to a GST antibody chip in the presence of 5 μM Iβ1A or 0.05% DMSO. Binding of importin β at various concentrations in the presence of 5 μM Iβ1A to GST-IBB. E) Noncovalently immobilized to a GST antibody chip. Black lines represent actual data collected in duplicates, and red lines are theoretical simulations derived from global fit on the data set.

no effect on the binding of importin β to either GST-IBB or GST-Nup153-C (Figure 7, panel E and Supplementary Figure S13, panel D), Iβ1A essentially abolished binding of importin β to GST-RanQ69LGTP, since with 1 μM importin β, an ~70% drop in response units was observed with 5 μM Iβ1A as compared to the DMSO control (Figure 7, panel D).

The strong inhibition of the interaction of importin β with RanGTP but not its interaction with the importin α IBB domain or with Nup153 by Iβ1A suggest that the most likely mechanism for inhibition of nuclear import by Iβ1A involves compromised dissociation of importin α/β/cargo complexes at the nuclear side of the NPC and a failure in cargo unloading into the nucleus, since these critically depend on binding of RanGTP to importin β (*33*). However, we cannot rule out other effects involving the binding of RanGTP to importin β, such as importin β recycling to the cytoplasm.

In summary, using confocal nanoscanning we have identified several structurally related novel small-molecule inhibitors for importin β mediated nuclear import that will provide valuable tools for further investigations. Our *in vitro* and *in vivo* results with Iβ1A are of particular importance as, along with peptidomimetic

inhibitors recently identified in our laboratory (Ambrus, G.; Whitby, L. R.; Singer, E. L. *et al.*, unpublished data), they provide the first *bona fide* small molecule inhibitor of importin α/β mediated import and establish the chemical druggability of the importin β pathway for inducing biological effects. We suggest naming these nuclear transport inhibitors karyostatins and have therefore have designated Iβ1A, the prototype of importin β inhibitors, as karyostatin 1A. Future work will be directed toward optimization of these compounds. The currently available set of compounds, although containing valuable SAR information, shows a suboptimal behavior in cellular assays due to the rather hydrophobic nature of AIDA as well as some of the building block combinations. Truncation of the compounds at the less sensitive positions and replacement of AIDA by less extended hydrophobic heterocycles may lead to further optimized compounds with better efficacy in cellular assays

METHODS

On-Bead Screening by Confocal Nanoscanning and Bead Picking. A detailed description of the PS02 instrument and its application for on-bead screening by automated confocal nanoscanning has recently been published (*9*). For library screening, 1 mg of beads from the respective sublibraries were placed in 1.5-mL tubes (Eppendorf) and swollen in 200 μL of screening buffer, containing 20 mM Hepes pH 7.4, 110 mM potassium acetate, 2 mM magnesium acetate, 0.2 mM DTT, 0.1 mM CHAPS, 2% DMSO 2% (v/v), 2% acetonitrile 2% (v/v), 0.1% pluronic (w/v) (Molecular Probes), 0.2% BSA (w/v) (Sigma). The samples were then vortexed, the remaining bead clusters were broken up by a short sonication, and the beads were transferred to the wells of 96-well microtiter plate. The samples were incubated for 1 h with 200 μL of screening buffer containing 60 nM Alexa488 labeled importin β under constant agitation. After that the beads were left to settle for 1 min to form a monolayer at the well bottom of the microtiter plate was placed on the sample holder of the PS02 instrument. Confocal nanoscanning was performed at 5 μm resolution, the confocal scan height was set to 25 μm above the well bottom, and the scanning was performed using the appropriate instrumental settings and filter sets for Alexa488 (488 nm argon ion laser excitation, dichroic mirror 565DRLP, and emission filter 535RDF50).

The acquired scan images were quantitatively analyzed using the instrument's BeadEval software (Perkin-Elmer) and the beads were ranked according to their fluorescence ring intensities according to previously published procedures (*9*). Finally, the beads with the highest fluorescent ring intensities were isolated using the PS02's bead picking device and placed into autosampler glass vials (8002-SC-H/i3μ, Glastechnik Gräfenroda).

Cleavage of Isolated Hit Compounds by Photolysis. For photolysis, 40 μL of 1% TFA/methanol (Merck) was added to each vial, and the closed vials were placed in a Stratalinker 1800 UV illumination cabinet (Stratagene) and exposed for 120 min to 365 nm UV illumination at a power of 1070 μJ min^{-1}. After photolysis, the solvents were removed under vacuum, and the compounds redissolved in 5 μL of 30% acetonitrile in water, containing 0.1% TFA for μHPLC/MS analysis.

MS Analysis and Decoding of Hit Structures. The samples were analyzed on a μHPLC/MS instrument, consisting of a HP1100 HPLC system (Hewlett-Packard), equipped with a 30-nL flow cell UV detector (LC Packings) set to 214 nm and a LCQ ion trap mass spectrometer (Finnigan Corp) operated in MS mode for mass determination and in CID dependent scan mode for fragmentation of selected ions.

A 2.5-μL portion of each sample was injected and analyzed on a Hypersil C18 (5 μm, 150 mm × 0.8 mm) column (Lc Packings) at a flow rate of 100 μL min^{-1} and with a linear gradient from 10% to 95% acetonitrile in water containing 0.1% TFA over 15 min. The analytes were passed into the electrospray source of the LCQ *via* a fused silica capillary (340 μm o.d. × 50 μm i.d.). The source was operated at 4.5 kV with the heated capillary set at 220 °C and sheath nitrogen gas flow rate at 80. In the MS mode the ion time was set at 500 ms and the target number of ions at 5×10^7; in the CID mode the ion time was at 500 ms and the target number of ions at 210^7. In both modes 3 microscans per spectrum were performed. The electron multiplier was set at −1000 V, and all spectra were collected in the positive-ion mode.

Mass spectra analysis and interpretation of the individual LC separated peaks was performed using the Xcalibur software (Thermo Finnigan, Version1.3). After identification of the monoisotopic mass of the apparent end product, structures were assigned using a look-up table containing the expected molecular masses as well as masses for the expected MS-fragments for each library compound.

Affinity Measurements of AIDA-Tagged Hit Compounds in Solution. For affinity measurements in homogeneous solution, the AIDA tagged hit compounds were dissolved in DMSO and subsequently diluted into assay buffer (20 mM Hepes pH 7.4, 110 mM potassium acetate, 2 mM magnesium acetate, 0.2 mM DTT, 0.1 mM CHAPS), keeping the final DMSO concentration at 5%. The titration of AIDA compounds were performed on a SPEX Fluorolog τ3 spectrofluorometer in quartz cuvettes with 2 mm thickness and 10 mm path length (Hellma, 119.004F-QS) at 25 °C. The polarization measurements (titrations) of the AIDA-tagged compounds were performed at excitation and emission wavelengths set to 336 and 397 nm, respectively, using magic angle settings and an excitation bandwidth of 5 nm. The voltage of the emission channel PMTs was set to 950 V. A WG345 longpass filter was used in the emission channel to reduce straylight influences. Measurements were performed in T-format. For each titration point, a cycle of 3 measurements was performed. Each cycle consisted of 9 repeated measurements at vertically and horizontally oriented polarizers with an integration time of 5 s. The iteration limit for the calculated anisotropy was set to 0.1%. The samples were titrated by adding increasing amounts of importin β into a solution containing ~50 nM of AIDA tagged compound. Equilibrium dissociation constants (K_d values) were obtained by performing a nonlinear least-squares regression fit of the anisotropy data sets, with the software package GraFit 5.0 and assuming a 1:1 binding model.

Nuclear Import Assay Using Permeabilized Cells. Nuclear import assays using permeabilized cells were carried out essentially as previously described (*34*). See Supporting Information for more details.

Nuclear Import Assay in Living Cells Using Stably Transfected HeLa Cells. The *in vivo* nuclear transport assay with GFP-NFAT stably transfected into HeLa cells was carried out essentially as described before (*26, 27*). See Supporting Information for more detail.

Protein Expression and Purification. Expression and purification of importin β, importin α, Ran, NTF2, transportin, M9-nucloplasmin (*35*), GST-IBB, GST-RanQ69L, and GST-Nup153 (*34*) has been described previously (*25, 36*). GTP loading of GSTRanQ69L was carried out as described earlier. FITC-BSA-NLS (*36*) and FITC-M9-nucloplasmin (*35*) cargo coupling and labeling was done following previously published methods.

Surface Plasmon Resonance Measurements. Surface plasmon resonance experiments were carried out essentially as described previously (*30*). See Supporting Information for more detail.

Compound Characterization. For compound characterization see Supporting Information.

Acknowledgment: The authors would like to thank Gino Cingolani for his advice on surface plasmon resonance measurements. This work was supported by National Institutes of Health grants GM041955 and NS059460 to L.G. and CHRP postdoctoral fellowship F07-SRI-214 to G.A.

Supporting Information Available: This material is available free of charge *via* the Internet at http://pubs.acs.org.

REFERENCES

1. Terry, L. J., Shows, E. B., and Wente, S. R. (2007) Crossing the nuclear envelope: hierarchical regulation of nucleocytoplasmic transport, *Science 318*, 1412–1416.
2. Stewart, M. (2007) Molecular mechanism of the nuclear protein import cycle, *Nat. Rev. Mol. Cell. Biol. 8*, 195–208.
3. Weis, K. (1998) Importins and exportins: how to get in and out of the nucleus, *Trends Biochem. Sci. 23*, 185–189.
4. Cook, A., Bono, F., Jinek, M., and Conti, E. (2007) Structural biology of nucleocytoplasmic transport, *Annu. Rev. Biochem. 76*, 647–671.
5. Bednenko, J., Cingolani, G., and Gerace, L. (2003) Nucleocytoplasmic transport: navigating the channel, *Traffic 4*, 127–135.
6. Gorlich, D., Henklein, P., Laskey, R. A., and Hartmann, E. (1996) A 41 amino acid motif in importin-alpha confers binding to importin-beta and hence transit into the nucleus, *EMBO J. 15*, 1810–1817.
7. Lee, S. J., Matsuura, Y., Liu, S. M., and Stewart, M. (2005) Structural basis for nuclear import complex dissociation by RanGTP, *Nature 435*, 693–696.
8. Nachury, M. V., and Weis, K. (1999) The direction of transport through the nuclear pore can be inverted, *Proc. Natl. Acad. Sci. U.S.A. 96*, 9622–9627.
9. Hintersteiner, M., Buehler, C., Uhl, V., Schmied, M., Muller, J., Kottig, K., and Auer, M. (2009) Confocal nanoscanning, bead picking (CONA): PickoScreen microscopes for automated and quantitative screening of one-bead one-compound libraries, *J. Comb. Chem. 11*, 886–894.
10. Kudo, N., Wolff, B., Sekimoto, T., Schreiner, E. P., Yoneda, Y., Yanagida, M., Horinouchi, S., and Yoshida, M. (1998) Leptomycin B inhibition of signal-mediated nuclear export by direct binding to CRM1, *Exp. Cell Res. 242*, 540–547.
11. Nishi, K., Yoshida, M., Fujiwara, D., Nishikawa, M., Horinouchi, S., and Beppu, T. (1994) Leptomycin B targets a regulatory cascade of crm1, a fission yeast nuclear protein, involved in control of higher order chromosome structure and gene expression, *J. Biol. Chem. 269*, 6320–6324.
12. Kwon, Y.-J., Genovesio, A., Kim, N. Y., Kim, H. C., Jung, S., David-Watine, B., Nehrbass, U., and Emans, N. (2007) High-content classification of nucleocytoplasmic import or export inhibitors, *J. Biomol. Screening 12*, 621–627.
13. Wolff, B., Sanglier, J. J., and Wang, Y. (1997) Leptomycin B is an inhibitor of nuclear export: inhibition of nucleo-cytoplasmic translocation of the human immunodeficiency virus type 1 (HIV-1) Rev protein and Rev-dependent mRNA, *Chem. Biol. 4*, 139–147.
14. Yashiroda, Y., and Yoshida, M. (2003) Nucleo-cytoplasmic transport of proteins as a target for therapeutic drugs, *Curr. Med. Chem. 10*, 741–748.
15. Kau, T. R., and Silver, P. A. (2003) Nuclear transport as a target for cell growth, *Drug Discovery Today 8*, 78–85.
16. Kobayashi, T., Kamitani, W., Zhang, G., Watanabe, M., Tomonaga, K., and Ikuta, K. (2001) Borna disease virus nucleoprotein requires both nuclear localization and export activities for viral nucleocytoplasmic shuttling, *J. Virol. 75*, 3404–3412.
17. Kumar, S., Saradhi, M., Chaturvedi, N. K., and Tyagi, R. K. (2006) Intracellular localization and nucleocytoplasmic trafficking of steroid receptors: an overview, *Mol. Cell. Endocrinol. 246*, 147–156.
18. Van Neck, T., Pannecouque, C., Vanstreels, E., Stevens, M., Dehaen, W., and Daelemans, D. (2008) Inhibition of the CRM1-mediated nucleocytoplasmic transport by N-azolylacrylates: Structure-activity relationship and mechanism of action, *Bioorg. Med. Chem. 16*, 9487–9497.
19. Kosugi, S., Hasebe, M., Entani, T., Takayama, S., Tomita, M., and Yanagawa, H. (2008) Design of peptide inhibitors for the importin alpha /beta nuclear import pathway by activity-based profiling, *Chem. Biol. (Cambridge, MA, U. S.) 15*, 940–949.
20. Meisner, N. C., Hintersteiner, M., Uhl, V., Weidemann, T., Schmied, M., Gstach, H., and Auer, M. (2004) The chemical hunt for the identification of drugable targets, *Curr. Opin. Chem. Biol. 8*, 424–431.
21. Meisner, N.-C., Hintersteiner, M., Seifert, J.-M., Bauer, R., Benoit Roger, M., Widmer, A., Schindler, T., Uhl, V., Lang, M., Gstach, H., and Auer, M. (2009) Terminal adenosyl transferase activity of post-transcriptional regulator HuR revealed by confocal on-bead screening, *J. Mol. Biol. 386*, 435–450.
22. Hintersteiner, M., and Auer, M. (2008) Single-bead, single-molecule, single-cell fluorescence technologies for drug screening and target validation, *Ann. N. Y. Acad. Sci. 1130*, 1–11.
23. Hintersteiner, M., Kimmerlin, T., Kalthoff, F., Stoeckli, M., Garavel, G., Seifert, J.-M., Meisner, N.-C., Uhl, V., Buehler, C., Weidemann, T., and Auer, M. (2009) Single bead labeling method for combining confocal fluorescence on-bead screening and solution validation of tagged one-bead one-compound libraries, *Chem. Biol. (Cambridge, MA, U. S.) 16*, 724–735.
24. Muckenschnabel, I., Falchetto, R., Mayr, L. M., and Filipuzzi, I. (2004) /1/15) SpeedScreen: label-free liquid chromatography-mass spectrometry-based high-throughput screening for the discovery of orphan protein ligands, *Anal. Biochem. 324*, 241–249.
25. Melchior, F., Sweet, D. J., and Gerace, L. (1995) Analysis of Ran/TC4 function in nuclear protein import, *Methods Enzymol. 257*, 279–291.
26. Kehlenbach, R. H., Dickmanns, A., Kehlenbach, A., Guan, T., and Gerace, L. (1999) A role for RanBP1 in the release of CRM1 from the nuclear pore complex in a terminal step of nuclear export, *J. Cell Biol. 145*, 645–657.
27. Kehlenbach, R. H., Dickmanns, A., and Gerace, L. (1998) Nucleocytoplasmic shuttling factors including Ran and CRM1 mediate nuclear export of NFAT In vitro, *J. Cell Biol. 141*, 863–874.
28. Bischoff, F. R., and Gorlich, D. (1997) RanBP1 is crucial for the release of RanGTP from importin beta-related nuclear transport factors, *FEBS Lett. 419*, 249–254.
29. Ben-Efraim, I., and Gerace, L. (2001) Gradient of increasing affinity of importin beta for nucleoporins along the pathway of nuclear import, *J. Cell Biol. 152*, 411–417.
30. Mitrousis, G., Olia, A. S., Walker-Kopp, N., and Cingolani, G. (2008) Molecular basis for the recognition of snurportin 1 by importin beta, *J. Biol. Chem. 283*, 7877–7884.
31. Adam, S. A., and Gerace, L. (1991) Cytosolic proteins that specifically bind nuclear location signals are receptors for nuclear import, *Cell 66*, 837–847.

32. Adam, E. J., and Adam, S. A. (1994) Identification of cytosolic factors required for nuclear location sequence-mediated binding to the nuclear envelope, *J. Cell Biol. 125*, 547–555.
33. Kutay, U., Izaurralde, E., Bischoff, F. R., Mattaj, I. W., and Gorlich, D. (1997) Dominant-negative mutants of importin-beta block multiple pathways of import and export through the nuclear pore complex, *EMBO J. 16*, 1153–1163.
34. Bednenko, J., Cingolani, G., and Gerace, L. (2003) Importin beta contains a COOH-terminal nucleoporin binding region important for nuclear transport, *J. Cell Biol. 162*, 391–401.
35. Melchior, F., Paschal, B., Evans, J., and Gerace, L. (1993) Inhibition of nuclear protein import by nonhydrolyzable analogues of GTP and identification of the small GTPase Ran/TC4 as an essential transport factor, *J. Cell Biol. 123*, 1649–1659.
36. Cassany, A., and Gerace, L. (2009) Reconstitution of nuclear import in permeabilized cells, *Methods Mol. Biol. 464*, 181–205.